**Transepicondylar Distance Can Predict Graft and Tunnel Length for Different Pediatric Anterior Cruciate Ligament Reconstruction Techniques: A Magnetic Resonance Imaging Study**

Rosso F, Rossi R, Cantivalli A, Davico M, Fracassi M, Carnazza G, Bonasia DE. Transepicondylar Distance Can Predict Graft and Tunnel Length for Different Pediatric Anterior Cruciate Ligament Reconstruction Techniques: A Magnetic Resonance Imaging Study. Arthroscopy. 2022 Apr;38(4):1239-1251.e3. doi: 10.1016/j.arthro.2021.08.011. Epub 2021 Aug 21. PMID: 34425207.

# Transepicondylar Distance Can Predict Graft and Tunnel Length for Different Pediatric Anterior Cruciate Ligament Reconstruction Techniques: A Magnetic Resonance Imaging Study

Federica Rosso 1, Roberto Rossi 2, Antonino Cantivalli 2, Marco Davico 3, Matteo Fracassi 3, Gino Carnazza 3, Davide Edoardo Bonasia 2

1AO Ordine Mauriziano Hospital, Department of Orthopaedics and Traumatology, University of Torino, Torino, Italy. Electronic address: federica.rosso@yahoo.it.

2AO Ordine Mauriziano Hospital, Department of Orthopaedics and Traumatology, University of Torino, Torino, Italy.

3J Medical Sports Clinic, Torino, Italy.

**Abstract**

**Purpose**

To find a correlation and mathematical formulas between a linear 2-dimensional (2D) magnetic resonance imaging (MRI) measurement around the knee and the length of the grafts and tunnels required for both all-inside-all-epiphyseal and Kocher–Micheli pediatric anterior cruciate ligament (ACL) reconstruction techniques.

**Methods**

At time 0 and 30 days after, 2 observers measured: (1) on standard 2D knee MRI, 7 linear distances, representing morphologic measurements, such as transepicondylar distance (TD), and (2) on 3-dimensional (3D) MRI, 5 curved distances, corresponding to Kocher–Micheli and all-epiphyseal ACL reconstruction techniques. Intra- and interobserver reliability was tested for all measurements. The correlation between 2D and 3D measurements was tested. The 2D measurement with highest repeatability and reproducibility and with strongest correlation with 3D measurements was used to extract formulas to calculate the tunnel and graft length for the 2 techniques.

**Results**

Seventy-six MRIs were used. The intra- and interobserver reliability of 2D measurement was high, with TD showing the highest reproducibility and repeatability. 3D measurements also

showed good intra and inter-observer reliability. A linear correlation was found between 2D and 3D measurements, with TD showing the strongest correlation. TD was used to extract formulas to calculate graft or tunnel length for Kocher–Micheli and all-epiphyseal ACL reconstruction. All formulas were proven to be accurate. A *reference chart* was also created to be used in the surgical setting.

**Conclusions**

With specific formulas, TD can be used to calculate the length of the tunnels, intra-articular portion and graft length for an all-inside all-epiphyseal pediatric ACL reconstruction and the length of the iliotibial band required for the Kocher–Micheli technique.

**Clinical Relevance**

The surgeon can use these formulas in pediatric ACL reconstruction preoperative planning, graft harvesting and tunnel drilling.

Anterior cruciate ligament (ACL) injuries in pediatric patients are increasing, with an annual incidence ranging from 50.9 to 76 per 100,000 people aged 3 to 20 years.[1-3] ACL injuries account for 30% of all knee injuries in children and adolescents between 5 and 18 years of age.[4,5] Conservative treatment and delayed ACL reconstruction have shown poor outcomes with a high risk of meniscal and chondral injuries as well as a 50% sport dropout rate.[1,6] Based on the patients' age and growth potential, different physeal-sparing or physeal-respecting ACL-reconstruction techniques have been developed for the pediatric population, with the most common being (1) Kocher–Micheli,[7] (2) all-epiphyseal,[1] (3) partial transphyseal (transphyseal on the tibial side and physeal sparing on the femur),[8,9] and (4) transphyseal.[10]

The dimensions of the knee can range widely between patients with open physes, resulting in a significant variability of tunnel and graft length required for different reconstruction techniques. In all-inside all-epiphyseal pediatric ACL reconstruction, one femoral and one tibial socket are drilled in the distal femoral and proximal tibial epiphysis; therefore, the length of the tunnels as well as the intra-articular portion of the ACL can significantly influence the length of the graft required for the reconstruction. Indeed, a graft–tunnel mismatch should be avoided with this technique, since a too-long graft can result in a lax ligament and a too-short graft might not seat properly in the sockets, with poor tendon–bone integration. Therefore, knowing preoperatively the length of the sockets and graft could be useful for the surgeons performing all-epiphyseal pediatric ACL reconstruction.

In the Kocher–Micheli pediatric ACL-reconstruction technique, a strip of the iliotibial band (ITB) is harvested, left attached distally on the Gerdy's tubercle, passed in an over-the-top position on the femur, under the intermeniscal ligament, and then fixed to the anteromedial tibia. This technique as well as knowing preoperatively the length of the graft required for the reconstruction can help the surgeon in avoiding redundant ITB harvest and minimizing invasiveness on the lateral thigh.

Measuring the length of the graft and tunnels needed for pediatric ACL reconstruction on standard 2-dimensional (2D) magnetic resonance imaging (MRI) is not possible. Two-dimensional MRI allows only for 2D measurements, i.e., a linear segment from A to B, with A and B lying on the same MRI cut. In contrast, high-quality isotropic 3-dimensional (3D) MRI

sequences allow for a 3D reconstruction and multiplanar reformatting.[11] With 3D MRI, every type of measurement can be made (i.e., the distance of 2 or more points, linear or curved, with the points lying on the same cut or different cuts), including the length of the graft needed for complex ACL-reconstruction techniques. However, most protocols for knee MRI only include 2D sequences and not 3D isotropic sequences because of the following reasons: (1) 3D MRI requires a longer acquisition time compared with 2D sequences; (2) due to the longer acquisition time, 3D isotropic sequences are more susceptible to motion artifacts, particularly in children; and (3) the sensitivity of 3D MRI for meniscal and ACL injuries seems to be lower than 2D MRI, because of image blurring, decreased in-plane resolution, and suboptimal soft-tissue contrast.[12,13]

As a result of 3D MRI not being included in standard knee protocols, direct measurement of tunnel and graft length required for pediatric ACL reconstruction techniques is not possible in the clinical practice. The main goal of this study was to find a correlation and mathematical formulas between a linear 2D MRI measurement around the knee and the length of the grafts and tunnels required for both all-inside-all-epiphyseal and Kocher–Micheli pediatric ACL-reconstruction techniques.

In this descriptive laboratory study, the author's hypotheses were that (1) the transepicondylar distance (TD) will show the greatest reliability, repeatability and correlation with 3D measurements and (2) different formulas can be obtained to predict the length of the grafts and tunnels for pediatric ACL reconstruction, using the TD.

**Methods**

This study was approved by the local ethical committee (AO Città della Salute e della Scienza, protocol number 0099939). The images of all patients younger than 14 years of age who received a knee MRI at the J Medical Sports Clinic (Torino) from November 2016 to November 2019 were evaluated. Exclusion criteria were (1) closed physes; (2) congenital/hereditary diseases causing articular deformities (i.e., spondyloepiphyseal dysplasia, congenital patellar dislocation, etc.); (3) previous knee surgeries; (4) chronic inflammatory diseases; (5) presence of hardware in the knee; (6) previous tibial, femoral, patellar fractures; and (7) unavailable 3D MRI sequences.

All images were acquired with a 1.5-T MRI scanner (Optima MR450w 1.5T GEM; GE Healthcare, Milwaukee, WI) and an 8-channel knee coil (Invivo 1.5 HD T/R).

Routine 2D sagittal proton-density weighted (PDw)-fast spin echo (FSE) and PDw-FSE fat suppression images, axial T2w-FSE images, and coronal PDw-FSE fat suppression images and 3D PDw-FSE fat suppression images with isotropic voxel (CUBE, 0.6 × 0.6 × 0.6 mm) were acquired in each patient. The acquisition time was 10 minutes for the entire 2D MRI protocol and 5 minutes for the sagittal CUBE sequence. The sagittal source images from the 3D CUBE technique were used to create sagittal, coronal, and axial reformatted images of the knee joint. The reformatted images were used for the 3D CUBE assessment of the knee. The postprocessing of the 3D CUBE sequence was performed by a radiologist on a GE Healthcare MRI Advantage workstation 4.7 (Milwaukee, WI) after acquisition of the images.

Two sports medicine fellowship–trained orthopaedic surgeons (D.E.B. and F.R.) performed the 2D and 3D measurements at time 0 (T0) and after 30 days (T1) on OsiriX DICOM viewer (Pixmeo, Bernex, Switzerland).

**2D Measurements**

To decide the 2D measurements to be included in the study, 2 sports medicine fellowship–trained orthopaedic surgeons (D.E.B. and F.R.) were asked the following question:

Based on the recent literature and your experience, which 2D measurements having the following characteristics would you include in this study?

•

morphologic measurements of the knee joint (bone or soft tissue) that can potentially affect the length of the tunnels and graft required for different pediatric ACL reconstruction techniques;

•

measurements obtainable on standard 2D MRI protocols; or

•

measurements easy to perform in the clinical practice (with simple or no instructions to be provided to clinicians).

After discussion, the 2 surgeons agreed on the following measurements to be included[14-16] (Fig 1):

1)

TD: defined as the longest distance between the apices of the medial and lateral femoral epicondyles in the mediolateral axis, measured on axial cuts.

2)

Proximal tibia mediolateral dimension: defined as the longest mediolateral dimension of the proximal tibial in the mediolateral axis, measured on proximal axial cuts just distal to the menisci and parallel to the posterior tibial condylar axis.

3)

Tibial plateau anteroposterior dimension: defined as a segment drawn from the center of the posterior cruciate ligament tibial insertion and the anterior tibial cortex aiming the center of the patellar tendon, measured on axial cuts.

4)

Lateral femoral condyle anteroposterior dimension: defined as the longest dimension of the lateral femoral condyle tangential to the distal femoral physis in the anteroposterior axis, measured on sagittal cuts.

5)

Lateral femoral condyle mediolateral dimension: defined as the longest mediolateral dimension of the lateral femoral condyle, measured on coronal cuts, parallel to the joint line and midpoint between the articular cartilage and the distal femoral physis.

6)

Lateral femoral condyle craniocaudal dimension: defined as the longest craniocaudal dimension of the lateral femoral condyle from the distal femoral physis to the articular cartilage, measured on coronal cuts, perpendicular to the joint line.

7)

Medial femoral condyle craniocaudal dimension: defined as the longest craniocaudal dimension of the medial femoral condyle from the distal femoral physis to the articular cartilage, measured on coronal cuts, perpendicular to the joint line.

The observers were intentionally not instructed regarding the weighting of the sequence for 2D measurements, for possible subsequent application in the clinical setting. The articular cartilage and the periosteum were excluded from the measurements.

3D Measurements

The 3D measurements were performed on the 3D MRI sequences by the same observers at time 0 (T0) and after 30 days (T1). The 3D measurements corresponded to (1) the Kocher–Micheli and (2) the all-epiphyseal pediatric ACL reconstruction techniques.

1.

Kocher–Micheli technique: defined as the ACL graft path of the Kocher-Micheli technique, starting from the center of the Gerdy's tubercle, passing along the lateral femoral condyle, entering the joint with an over-the-top position, passing under the intermeniscal ligament and ending on the anteromedial aspect of the tibia just distal to the physis (Fig 2).

2.

All-epiphyseal pediatric ACL reconstruction. During this measurement, observers were asked to measure the femoral tunnel, tibial tunnel and intra-articular portion of the ACL separately. Observers were also asked to simulate in the distal femoral and proximal tibial epiphyses the longest possible tunnels, which could be reproduced in the surgical setting without damaging the growth plates or other relevant structures (i.e., lateral collateral ligament, popliteus tendon, medial collateral ligament). The measurements included (Figs 3, 4 and 5) were as follo)

Femoral full tunnel (FFT): defined as the distance from the center of the femoral ACL footprint to the lateral femoral cortex (longest possible tunnel, reproduceable in the surgical setting without damaging the growth plates or other relevant structures).

2)

Intra-articular length of the graft: defined as the distance from the center of the tibial ACL footprint to the center of the femoral footprint

3)

Tibial full tunnel (TFT): defined as the distance from the center of the tibial ACL footprint to the anteromedial tibial cortex (longest possible tunnel, reproduceable in the surgical setting without damaging the growth plates or other relevant structures).

4)

Femoral tunnel – femoral physis distance: defined as the distance between the femoral tunnel and the most distal portion of the distal femoral physis measured in the coronal plane

5)

Femoral tunnel – lateral femoral epicondyle distance: defined as the distance between the femoral tunnel and the lateral femoral epicondyle measured in the coronal plane.

In addition, the orientation of the tibial and femoral tunnels has been measured in the coronal and axial planes, including:

•

Femoral tunnel / joint line angle: defined as the angle between the femoral tunnel and the joint line measured in the coronal plane.

•

Femoral tunnel / posterior condylar axis angle: defined as the angle between the femoral tunnel and the posterior femoral condylar axis measured in the axial plane.

•

Tibial tunnel / joint line angle: defined as the angle between the tibial tunnel and the joint line measured in the coronal plane.

•

Tibial tunnel / posterior condylar axis angle: defined as the angle between the tibial tunnel and the posterior femoral condylar axis measured in the axial plane.

Please note that, in the surgical setting of an all-inside all-epiphyseal pediatric ACL reconstruction, these measurements for the tibial and femoral tunnels corresponded to the full 4.5-mm tunnel and not the sockets (Fig 5). The length of the tibial socket (TS) and femoral socket (FS) was calculated with the following trigonometric formula:

$TS = TFT - [5/\mathrm{TAN}(\mathrm{TTPDI})]$

$FS = \mathrm{FFT}-[5/\mathrm{TAN}(\mathrm{FTPDI})]$

This formula was used to obtain the longest socket possible without damaging the distal femoral and proximal tibial physes, when retrodrilling with a 10-mm diameter reamer.

**Statistical Analysis**

The number of knees (76) was deemed appropriate since the minimum number of samples required for reliability studies is 42 (sample size calculation with $\alpha = 0.05$, $\beta = 0.2$, $\rho(0) = 0.6$, $\rho(10) = 0.85$).[17]

Data are reported with mean, standard deviation (SD), and/or ranges. The normality of the distribution of the measurements was tested with the D'Agostino–-Pearson test. The intraobserver reliability was tested with the Pearson correlation index (*r)* in case of normal distribution or the Spearman rank correlation coefficient (rho), for not normal distribution, together with the Cronbach alpha coefficient. The interobserver reliability was tested with the Cronbach alpha coefficient and Intraclass correlation coefficient (ICC). In addition, the correlation between the 2D measurements and the 3D measurements was tested with the Pearson correlation index (all data showed normal distribution). The 2D measurement with greatest intra- and interobserver reliability and with the strongest correlation with 3D measurements (length of the different reconstruction techniques) was used to extract formulas to calculate the 3D measurements from 2D values. The formulas were obtained with linear regression. In addition, the accuracy of the 3D measurements obtained with the formulas was compared with the same measurements directly performed on the 3D MRI, using paired the *t* test and Bland–Altman plots. Statistics was performed with MedCalc Statistical Software version 16.4.3 (MedCalc Software, Ostend, Belgium).

**Results**

**Patients' Demographics**

Ninety-one patients were firstly included in the study (91 knees). Fifteen patients were excluded due to (1) closed physes (6 patients); (2) congenital patellar dislocation (1 patient); (3) previous knee surgery (4 patients); (4) presence of hardware in the knee (1 patient); and (5) unavailable 3D MRI sequences (3 patients).

Seventy-six patients (76 knees) were finally included in the study, 48 (63%) were boys, and the mean age was 12.6 years (SD 1.49, range 8.4-13.9 years). The right knee was studied in 42 patients (55%).

The average distance from the center of the femoral tunnel to the center of lateral epicondyle and the distal femoral physis were 10.7 mm (SD 1.97) and 10 mm (SD 1.91), respectively. This information can be useful in the surgical setting: the surgeon can assume that the most distal portion of the lateral femoral physis is approximately at the same level of the lateral epicondyle.

Averages and SDs for all measurements are reported in Appendix Table 1, available at www.arthroscopyjournal.org

, showing that the difference in terms of graft and tunnel length between small and large knees were significant. This difference was about 1 cm for the femoral tunnel and 1.5 cm for the tibial tunnel and intra-articular portion of the ACL. These differences summed up to 4 cm

when considering the entire all-epiphyseal ACL reconstruction between small and large knees. With the Kocher–Micheli technique, the length of the graft required varied up to 7 cm between small and large knees.

The femoral tunnel / joint line angle was 0° for both observers. As a matter of fact, both observers noted that inclining the tunnel from proximal (lateral cortex aperture of the tunnel) to distal (intra-articular aperture) did not guarantee preservation of the distal femoral physis in almost all patients. The longest FS was then assumed to be equal to the femoral tunnel minus 5 mm (Fig 5). The femoral tunnel / posterior condylar axis angle was on average 15.6° (SD 3°) with a direction from anterior (lateral cortex aperture of the tunnel) to posterior (intra-articular aperture). The FFT lateral cortex aperture was located on average 10 mm distal to the center of the lateral epicondyle.

The tibial tunnel / joint line angle was on average 33.8° (SD 4.1°) with a direction from medial (medial cortex aperture of the tunnel) to lateral (intra-articular aperture) and the tibial tunnel / posterior condylar axis angle was 9.5° (SD 5.3°) with a direction from posterior (medial cortex aperture of the tunnel) to anterior (intra-articular aperture). The TFT medial cortex aperture was located just anterior to the medial collateral ligament and immediately above the proximal tibial physis.

**Intraobserver Reliability**

The intraobserver reliability (Pearson or Spearman correlation according to the normality of the data distribution and Cronbach alpha) for the 2D and 3D measurements is summarized in Appendix Table 1, available at www.arthroscopyjournal.org

. Among the 2D measurements, the greatest intraobserver reliability was found for the TD for both observers (Pearson, Spearman, and Cronbach alpha >0.9).

**Interobserver Reliability**

The interobserver reliability tested with ICC and Cronbach alpha for the 2D and 3D measurements is shown in Appendix Table 1, available att www.arthroscopyjournal.org

. The second measurement (T1) of each observer was used for every test. Among the 2D measurements, the greatest interobserver reliability was found for the TD one more time (ICC and Cronbach's alpha >0.98).

**Correlation Between 2D and 3D Measurements**

The correlation between 2D measurements (independent variables) and 3D measurements (dependent variables) is shown in Appendix Table 2, available at

.

All independent variables were strongly correlated with the dependent variables (3D measurements). The TD showed the strongest correlation with all dependent variables, except one (tibial tunnel) where it turned out to be the second strongest.

**Linear Regression and Mathematical Formulas**

Simple linear regression was used to develop mathematical formulas able to calculate the 3D measurements (Y variable) from the TD (X variable). The TD was chosen among all the other 2D measurements because of its highest repeatability, reproducibility, and strongest correlation with 3D measurements. A linear correlation was found between the TD and all 3D measurements. Figure 6 shows the graphical results of the linear regression.

The following formulas were extracted to calculate the 3D measurements from the TD, with the result expressed in millimeters:

FFT = 5.05+(0.36xTD)

FS = 0.05+(0.36xTD)

IAGL = 4.85+ (0.34xTD)

TFT = 9.43+(0.32x TD)

TS= (0.37 x TD) -1.04

Kocher – Micheli = 11.23+(2.29x TD)

FFT + IAGL + TFT =16.47+ (1.43x TD)

Accuracy of the Formulas

The paired t test, used to assessed the accuracy of the formulas, showed no difference between the 3D measurements performed on the MRI and calculated with the formulas: FFT, P = .83; FS, P = .83; IAGL, P = .34; TFT, P = .12; TS, P = .45; Kocher–Micheli, P = .79; FFT + IAGL + TFT, P = .93; FS + IAGL + TS, P = .76.

The 3D measurements performed on the MRI and calculated with the formulas were also compared with the Bland–Altman plot (Fig 7). The Bland–Altman plot,18,19 or difference plot, is a graphical method to compare 2 measuring techniques. With this method, the differences between the 2 techniques are plotted against the averages of the 2 techniques. In this study, since the formulas were obtained from the 3D measurements performed on the MRI, the means of the 2 measuring techniques are very similar and this is demonstrated by the mean difference close to 0 on the plots (central blue line on Fig 7).

Another advantage of the Bland–Altman plot in this type of studies is that investigators can interpret the limits of agreement to assess whether the agreement is acceptable based on what is clinically relevant or not. The limits of agreement are expected to include about 95% of the differences observed in the future. In this study, the acceptable range of agreement was defined a priori at ±3 mm for shorter measurements (IAGL, FFT, TFT, FHS, and THS), at ±5 mm

for all-epiphyseal reconstruction (FFT + IAGL + TFT and FHS + IAGL + THS), and from 0 mm to +10 mm for Kocher–Micheli technique. In fact, from the clinical point of view, an over- or underestimation of 3 mm can be acceptable for shorter measurements (i.e., femoral socket in an all-epiphyseal reconstruction). Similarly, an over- or underestimation of 5 mm can be acceptable for the total length of the all-epiphyseal ACL reconstruction (FFT + IAGL + THS and FS + IAGL + TS). In contrast, for longer reconstruction techniques (i.e., Kocher–Micheli) an underestimation of the graft length cannot be accepted, while an overestimation of the length does not represent a clinical problem in the surgical setting, i.e., a surgeon does not want a graft shorter than needed, but can always cut the remnant of a longer graft. Based on the Bland-Altman plots the formulas for the tunnels, intra-articular graft and all-epiphyseal reconstruction (FFT, FHS, IAGL, TFT, THS, "FFT + IAGL + TFT" and "FHS + IAGL + THS") were considered accurate. Conversely, according to the need of the surgeon 10 mm were added to the formula for Kocher–Micheli reconstruction.

In addition, the decimals of all formulas were rounded for easier clinical application. The final formulas were as follows:

FFT = 5 + (0.36 × TD)

FS = (0.36 × TD)

IAGL = 5 + (0.34 × TD)

TFT = 9 + (0.32 × TD)

TS = (0.37 × TD) –1

Kocher–Micheli = 21 + (2.29 × TD)

FFT + IAGL + TFT = 16 + (1.43 × TD)

FS + IAGL + TS = 4 + (1.07 × TD)

Based on the data from the present study, a reference chart was created for the surgical setting (Table 1). Patients were grouped based on 5-mm increments of the TD. Using this table, surgeons obtain the maximum drillable length of the tibial and femoral sockets without damaging the physes. In addition, surgeons can obtain the length of the graft required for the all-inside pediatric ACL reconstruction. This was calculated by subtracting 5 mm to the FS+IAGL+TS measurement, to avoid a too-long graft, resulting in a lax ACL. With the same table, surgeons can also calculate the length of the ITB (measured from the Gerdy's tubercle) required for a Kocher–Micheli procedure.

## Discussion

The main findings of the present study included the following: (1) the intra- and interobserver reliability of linear 2D measurement and curved 3D measurements on 3D MRI was high, with the TD showing the greatest reproducibility and repeatability. (2) A strong linear correlation was found between 2D and 3D measurements, with the TD showing the strongest correlation.

(3) The authors were able to extract formulas to calculate the length of the FFT, FS, IAGL, TFT, TS, Kocher–Micheli, FFT + IAGL + TFT, and FS + IAGL + TS (Table 1). Furthermore, the safest location and orientation of the femoral and tibial tunnels was described. The longest femoral tunnel drillable in the distal femoral epiphysis should be parallel to the joint line on the coronal plane and inclined anteriorly of 15°, with a direction from anterior (lateral cortex aperture of the tunnel) to posterior (intra-articular aperture). In addition, the FFT lateral cortex aperture should be located on average 10 mm distal to the center of the lateral epicondyle. The femoral tunnel created in this fashion is in a safe position (with a distance from the center of the tunnel to the post distal part of the femoral physis of about 10 mm). (6) The longest tibial tunnel drillable in the proximal tibial epiphysis should be inclined of about 34° on the coronal plane with a direction from medial (medial cortex aperture of the tunnel) to lateral (intra-articular aperture) and inclined of about 9° on the axial plane with a direction from posterior (medial cortex aperture of the tunnel) to anterior (intra-articular aperture). In addition, the TFT medial cortex aperture was located just anterior to the medial collateral ligament and immediately above the proximal tibial physis.

Several MRI studies described the normal anatomy of pediatric ACL, distal femoral, and proximal tibial physes together with their changes during growth. Lima et al.20 showed that the ACL length showed significant progressive growth, with the greatest values at 15 years of age for female patients and at 16.1 years for male patients. In addition, coronal and sagittal inclination of the ACL showed a significant progressive increase with age in both sexes, progressively verticalizing. The ACL area showed more pronounced growth (up to 11 years in girls and 12 years in boys), then stabilized (from 11 to 14 years in girls and from 12 to 15 years in boys), and then sustained a slight reduction. Similarly, Putur et al.21 showed that the orientation of the ACL in the pediatric population transitions from oblique and anteriorly attached on the tibia to more vertical and posteriorly attached as the patient reaches skeletal maturity; the length and width of the ACL increased in a predictable way, characterized by growth models presented by the authors. Davis et al. described the height of the proximal tibial epiphysis and width of the lateral femoral epiphysis in pubescent22 and prepubescent patients23 with the goal or correctly placing and orienting all-epiphyseal tunnels. Similar to our study, the authors described a femoral tunnel parallel to the joint line. However, the authors only used 2D MRIs for the measurements, did not test the safety of the femoral tunnel position (distance from the tunnel to the growth plate), and did not simulate the tibial tunnel. Ladenhauf et al.,24 in a 3D MRI study, described that the shape of the distal femoral physis was linear in the anterior part of the femur and more concave shape in the posterior aspect of the medial and lateral condyles.

Several MRI studies, some of them including also 3D reconstructions of the physes and epiphyses, evaluated the amount of physeal damage when performing transphyseal tunnel drilling with different angulations.25, 26, 27, 28 As evidence supporting the methodology of the present study, Swami et al.29 showed that ACL attachments can be reliably identified in 2D MRI and in 3D MRI.

A few MRI studies simulated tibial and femoral tunnels with the goal of obtaining clinically relevant information regarding all-epiphyseal tunnel placement and length.30, 31, 32, 33 Davis et al.30 reviewed 95 2D MRIs of patients with open physes, divided them in 2 groups

(group 1 = boys <13 years and girls <12 years; group 2 = boys 13-14 year old and girls 12-14 year old), with the goal of studying the proximal tibial physis and the all-epiphyseal tibial tunnel. The 2D images were imported on a commercial imaging viewer with a 3D postprocessing tool. The authors simulated an all-epiphyseal tibial tunnel, measuring its maximum oblique length, a "safe" physeal-sparing length, and the inclination of the tunnel (only on the sagittal plane). Significant differences were described between younger versus older cohort for the maximum oblique length and its angular trajectory (22.2 vs 23.8 mm; 42.0° vs 39.4°, respectively) and for the physeal-sparing length and its angular trajectory (19.4 vs 21.3 mm; 30.1° vs 28.2°, respectively). The authors concluded that the simulated tibial tunnel across the tibial epiphysis is shorter than previously believed. However, the orientation of the tunnel simulated by Davis et al.30 has little angulation on the coronal plane, resulting in a limited length of the tunnel itself. In our study, observers noted that the longest drillable tunnel in the tibial epiphysis had a very medial extra-articular aperture, resulting in a significantly longer TFT (mean 26.7 mm, range 18.6-33.8) compared with the study by Davis et al.30 Similar to Davis et al.,30 Swami et al.31 studied the anatomy of the proximal tibial physis and its mean maximum oblique length. The authors reported that the center of the ACL tibial attachment was consistently near 51% of the anteroposterior tibial diameter, the vertical height of the tibial epiphysis was about 16 mm, and that maximum oblique length from ACL attachment was about 30 mm, occurring at a mean angle of 50°. The limitations of this study are very similar to the one by Davis et al. (2D MRI and tibial tunnel vertically oriented on the coronal plane).30,31 In contrast, Xerogeanes et al.33 focused their MRI study on the all-epiphyseal femoral tunnel. The authors evaluated 2D MRIs of patients between 6 and 17 years of age and used a software to create 3D reconstruction of the knees with the goals of measuring the height of the lateral femoral condyle, simulating 2 different all-epiphyseal femoral tunnels (femoral ALC footprint-lateral epicondyle and femoral ACL footprint-popliteus tendon insertion), and measuring the length and the distance from the tunnel to the physis for both femoral tunnels. The authors found that the femoral tunnel expanding from the femoral ACL footprint to the popliteus tendon insertion resulted in a safer tunnel placement with respect to the distal femoral physis. The mean distance from the center of the preferred ACL tunnel to the distal femoral physis was 12 mm, independent of sex ($P = .94$) or age, and the shortest distance was 8 mm. The length of this proposed tunnel averaged 30.1 mm in boys and 27.4 mm in girls ($P < .001$), and it averaged 25.4mm at an age of 6 years and 29.7mm at an age of 17 years. Although Xerogeanes et al.33 did not use 3D MRIs and only studied possible femoral tunnels, their study has some similarities with the present study: the femoral tunnel proposed was very similar to ours in terms of orientation (parallel to the joint line), extra-articular aperture (distal to the lateral epicondyle) and length.

The position of the present study in the existing sports medicine literature is rather unique. The present paper studied 3D MRIs as opposed to 2D MRIs used in most of the papers cited previously. Measurements performed on 3D reconstructions of standard 2D MRIs are less accurate than measurements performed on acquired 3D sequences, with a margin of error of about 4 mm, representing the thickness of a single axial 2D MRI slice.29 The findings and methods of the present study are corroborated by recent articles. Tran et al.15 found a strong correlation between pediatric ACL length and TD in a 2D MRI study. Van Zyl et al.16 demonstrated that the TD measured on either MRI or AP radiograph could reliably estimate

ACL length in adult patients. Similar to the present study, the authors obtained a formula to calculate the length of ACL from the TD (ACL length = 0.31 × TD + 11.33). Although this formula looks different from the one described in our study (ACL length= 4.85 + 0.34 × TD) the results are practically identical.16 As another strength of the present study, both tibial and femoral all-epiphyseal tunnels were studied, and the measurements were performed for both full tunnels and sockets to provide the surgeons with information useful in the surgical setting. Knowing preoperatively the length of the tunnels and the intra-articular portion of the ACL can help the surgeon with tunnel drilling and the assistant with graft preparation, with the goal of avoiding graft-tunnel mismatch. Graft–tunnel mismatch in all-inside all-epiphyseal pediatric ACL reconstruction is a relevant intraoperative complication, which could result in a too-long and lax graft or a too-short graft not seating properly in the bone sockets. Since all-inside all-epiphyseal pediatric ACL reconstruction is not recommended in prepubescent patients with small knees, the authors also included the Kocher–Micheli technique in the present study. This technique has proven to be safe and produce good outcomes7 and represents a reliable alternative option in prepubescent patients with small knees. In these patients, drilling all-epiphyseal tunnels on the tibia, can result in short, very horizontal tunnels with large and oval intra-articular apertures. The length of the ITB graft required for the Kocher–Micheli technique can be calculated with the methods described in this study, in order to avoid harvesting of a redundant ITB strip and minimize the invasiveness on the lateral thigh.

## Limitations

This study has several limitations. First, the data were obtained from MRI measurements and not real knees. A second limitation is related to the ethnicity of the population studied (White), and significant morphologic differences have been described among patients of different races.14 As another limitation, 10-mm diameter sockets were simulated in this study and pediatric ACL grafts are rarely this large (usually 7-8 according to the patients age and height). However, the authors wanted to describe the scenario at most risk of growth plate damage. As a last limitation, even though this is a widely accepted methodology for inter-rater agreement studies, only two investigators performed the measurements and more differences could be found with more observers.

## Conclusions

With specific formulas, TD can be used to calculate the length of the tunnels, intra-articular portion and graft length for an all-inside all-epiphyseal pediatric ACL reconstruction and the length of the ITB required for the Kocher–Micheli technique.

## References

1. Cordasco FA, Mayer SW, Green DW. All-inside, all-

epiphyseal anterior cruciate ligament reconstruction in

skeletally immature athletes: Return to sport, incidence of

second surgery, and 2-year clinical outcomes. Am J Sports

Med 2017;45:856-863.
2. Nogaro MC, Abram SGF, Alvand A, Bottomley N, Jackson WFM, Price A. Paediatric and adolescent anterior cruciate ligament reconstruction surgery. Bone Joint J 2020;102-b:239-245.
3. Tepolt FA, Feldman L, Kocher MS. Trends in pediatric ACL reconstruction from the PHIS Database. J Pediatr Orthop 2018;38:e490-e494.
4. Lima FM, Debieux P, Aihara AY, et al. The development of the intercondylar notch in the pediatric population. Knee 2020;27:747-754.
5. Gornitzky AL, Lott A, Yellin JL, Fabricant PD, Lawrence JT, Ganley TJ. Sport-specific yearly risk and incidence of anterior cruciate ligament tears in high school athletes: A systematic review and meta-analysis. Am J Sports Med 2016;44:2716-2723.
6. Ramski DE, Kanj WW, Franklin CC, Baldwin KD, Ganley TJ. Anterior cruciate ligament tears in children and adolescents: A meta-analysis of nonoperative versus operative treatment. Am J Sports Med 2014;42:2769-2776.
7. Kocher MS, Garg S, Micheli LJ. Physeal sparing reconstruction of the anterior cruciate ligament in skeletally immature prepubescent children and adolescents. Surgical technique. J Bone Joint Surg Am 2006;88:283-293 (suppl 1 Pt 2).
8. Lo IK, Kirkley A, Fowler PJ, Miniaci A. The outcome of operatively treated anterior cruciate ligament disruptions in the skeletally immature child. Arthroscopy 1997;13: 627-634.
9. Nagai K, Rothrauff BB, Li RT, Fu FH. Over-the-top ACL

reconstruction restores anterior and rotatory knee laxity in skeletally immature individuals and revision settings. Knee Surg Sports Traumatol Arthrosc 2020;28:538-543.
10. Domzalski M, Karauda A, Grzegorzewski A, Lebiedzinski R, Zabierek S, Synder M. Anterior cruciate ligament reconstruction using the transphyseal technique in prepubescent athletes: Midterm, prospective evaluation of results. Arthroscopy 2016;32:1141-1146.
11. Shakoor D, Guermazi A, Kijowski R, et al. Diagnostic performance of three-dimensional mri for depicting cartilage defects in the knee: A meta-analysis. Radiology 2018;289:71-82.
12. Chagas-Neto FA, Nogueira-Barbosa MH, Lorenzato MM, Salim R, Kfuri-Junior M, Crema MD. Diagnostic performance of 3D TSE MRI versus 2D TSE MRI of the knee at 1.5 T, with prompt arthroscopic correlation, in the detection of meniscal and cruciate ligament tears. Radiol Bras 2016;49:69-74.
13. Kayfan S, Hlis R, Pezeshk P, et al. Three-dimensional and 3-Tesla MRI morphometry of knee meniscus in normal and pathologic state. Clin Anat 2021;34:143-153.
14. Kim TK, Phillips M, Bhandari M, Watson J, Malhotra R. What differences in morphologic features of the knee exist among patients of various races? A systematic review. Clin Orthop Relat Res 2017;475:170-182.
15. Tran EP, Dingel AB, Terhune EB, et al. Anterior cruciate ligament length in pediatric populations: An MRI study. Orthop J Sports Med 2021;9:23259671211002286.
16. Van Zyl R, Van Schoor AN, Du Toit PJ, et al. The association between anterior cruciate ligament length and

femoral epicondylar width measured on preoperative magnetic resonance imaging or radiograph. Sports Med Arthrosc Rehabil 2020;2:e23-e31.
17. Donner A, Eliasziw M. Sample size requirements for reliability studies. Stat Med 1987;6:441-448.
18. Bland JM, Altman DG. Statistical methods for assessing agreement between two methods of clinical measurement. Lancet 1986;1:307-310.
19. Bland JM, Altman DG. Measuring agreement in method comparison studies. Stat Methods Med Res 1999;8:135-160.
20. Lima FM, Debieux P, Astur DC, et al. The development of the anterior cruciate ligament in the paediatric population. Knee Surg Sports Traumatol Arthrosc 2019;27:3354-3363.
21. Putur DE, Slaven SE, Niu EL. ACL Growth with age in pediatric patients: An MRI study. J Pediatr Orthop 2020;40: 438-447.
22. Davis DL, Chen L, Young ST. Evaluation of epiphyses in the skeletally immature knee using magnetic resonance imaging: A pilot study to analyze parameters for anterior cruciate ligament reconstruction. Am J Sports Med 2013;41:1579-1585.
23. Davis DL, Chen L, Ehinger M. A study of epiphyses in the young prepubescent knee using magnetic resonance imaging: Evaluation of parameters for anterior cruciate ligament reconstruction. Orthop J Sports Med 2014;2: 2325967114530090.
24. Ladenhauf HN, Jones KJ, Potter HG, Nguyen JT, Green DW. Understanding the undulating pattern of the distal femoral growth plate: Implications for surgical procedures involving the pediatric knee: A descriptive MRI study. Knee 2020;27:315-323.

25. Shea KG, Grimm NL, Nichols FR, Jacobs JC Jr. Volumetric damage to the femoral physis during double-bundle posterior cruciate ligament reconstruction: A magnetic resonance imaging computer modeling study. Arthroscopy 2015;31:1102-1107.
26. Kercher J, Xerogeanes J, Tannenbaum A, Al-Hakim R, Black JC, Zhao J. Anterior cruciate ligament reconstruction in the skeletally immature: An anatomical study utilizing 3-dimensional magnetic resonance imaging reconstructions. J Pediatr Orthop 2009;29:124-129.
27. Shea KG, Apel PJ, Pfeiffer RP, Traughber PD. The anatomy of the proximal tibia in pediatric and adolescent patients: Implications for ACL reconstruction and prevention of physeal arrest. Knee Surg Sports Traumatol Arthrosc 2007;15:320-327.
28. Shea KG, Belzer J, Apel PJ, Nilsson K, Grimm NL, Pfeiffer RP. Volumetric injury of the physis during single-bundle anterior cruciate ligament reconstruction in children: A 3-dimensional study using magnetic resonance imaging. Arthroscopy 2009;25:1415-1422.
29. Swami VG, Cheng-Baron J, Hui C, Thompson RB, Jaremko JL. Reliability of 3D localisation of ACL attachments on MRI: Comparison using multi-planar 2D versus high-resolution 3D base sequences. Knee Surg Sports Traumatol Arthrosc 2015;23:1206-1214.
30. Davis DL, Almardawi R, Mitchell JW. Analysis of the tibial epiphysis in the skeletally immature knee using magnetic resonance imaging: An update of anatomic parameters pertinent to physeal-sparing anterior cruciate ligament reconstruction. Orthop J Sports Med 2016;4:

2325967116655313.
31. Swami VG, Mabee M, Hui C, Jaremko JL. MRI anatomy of the tibial ACL attachment and proximal epiphysis in a large population of skeletally immature knees: Reference parameters for planning anatomic physeal-sparing ACL reconstruction. Am J sports Med 2014;42:1644-1651.
32. Marchwiany DA, Lee C, Ghobrial P, Lawley R, Chudik SC. All-epiphyseal physeal-sparing anterior cruciate ligament reconstructive surgery: A study of 3-dimensional modeling to characterize a safe and reproducible surgical approach. Arthrosc Sports Med Rehabil 2020;2:e435-e442.
33. Xerogeanes JW, Hammond KE, Todd DC. Anatomic landmarks utilized for physeal-sparing, anatomic anterior cruciate ligament reconstruction: An MRI-based study. J Bone Joint Surg Am 2012;94:268-276.

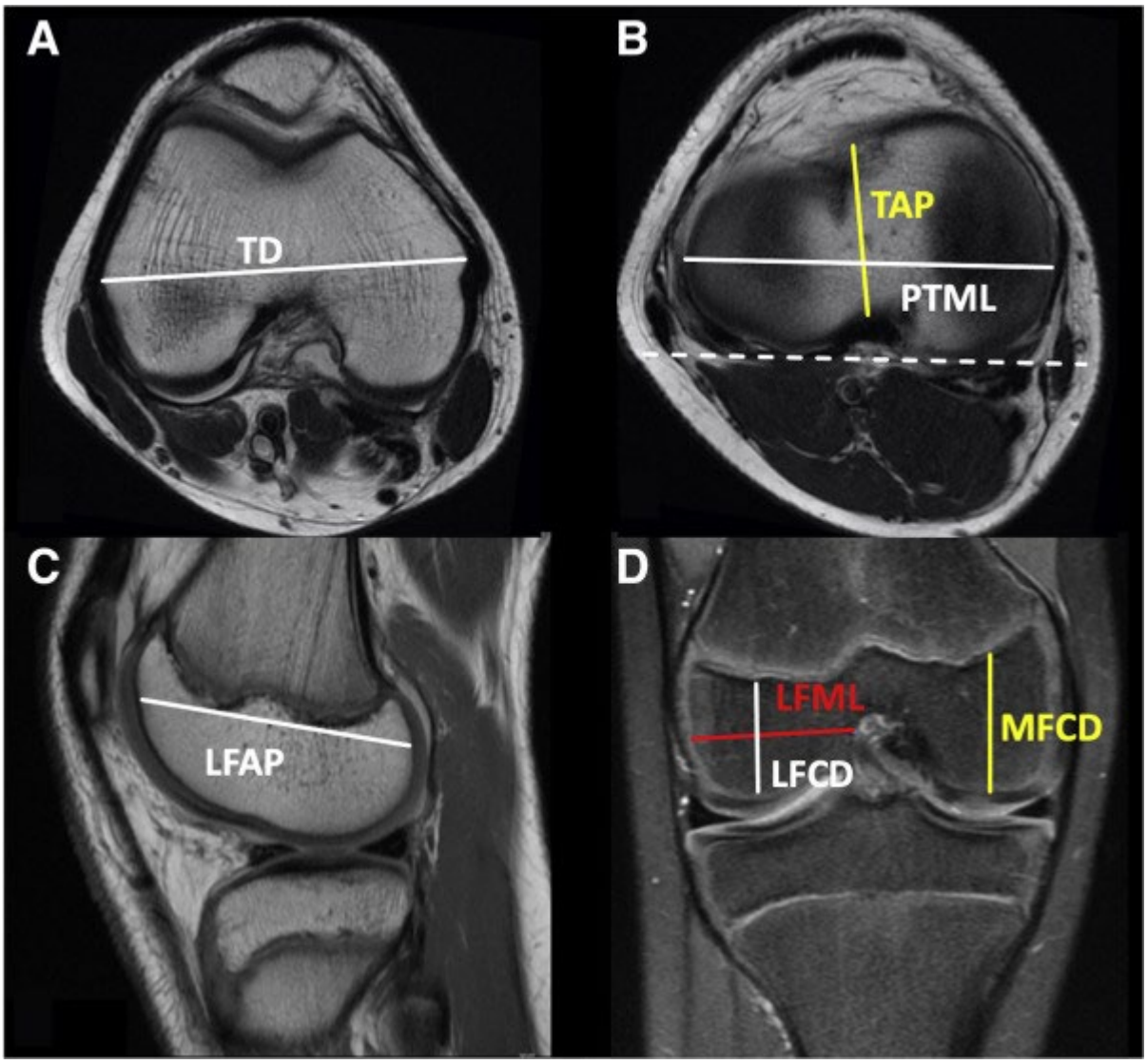


Fig 1. Two-dimensional (2D) measurements on 2D magnetic resonance imaging of a right knee: (A) transepicondylar distance (TD, white line), measured on axial cuts; (B) on axial the axial cuts, the proximal tibia mediolateral dimension (PTML, white line) parallel to the posterior tibial condylar axis (white dotted line), and the tibial plateau antero-posterior dimension (TAP, yellow line) were measured. (C) On the sagittal cuts, the lateral femoral condyle anteroposterior dimension (LFAP, white line) was measured. (D) On the coronal cuts, the lateral femoral condyle mediolateral dimension (LFML, red line), the lateral femoral condyle craniocaudal dimension (LFCD, white line), and the medial femoral condyle cranio-caudal dimension (MFCD, yellow line) were measured.

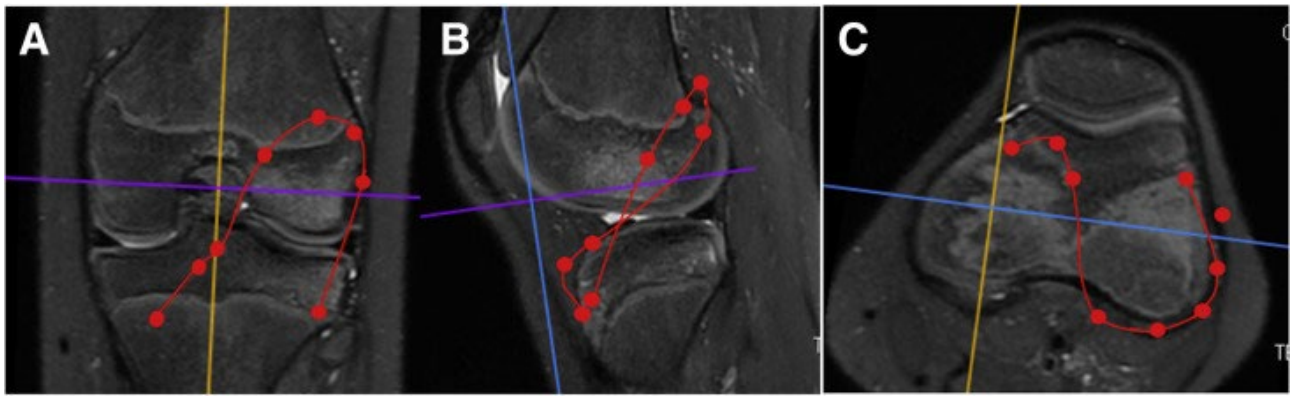


Fig 2. Three-dimensional (3D) measurement of the Kocher–Micheli technique on 3D magnetic resonance imaging sequences of a left knee. (A) coronal plane, (B) sagittal plane, and (C) axial plane.

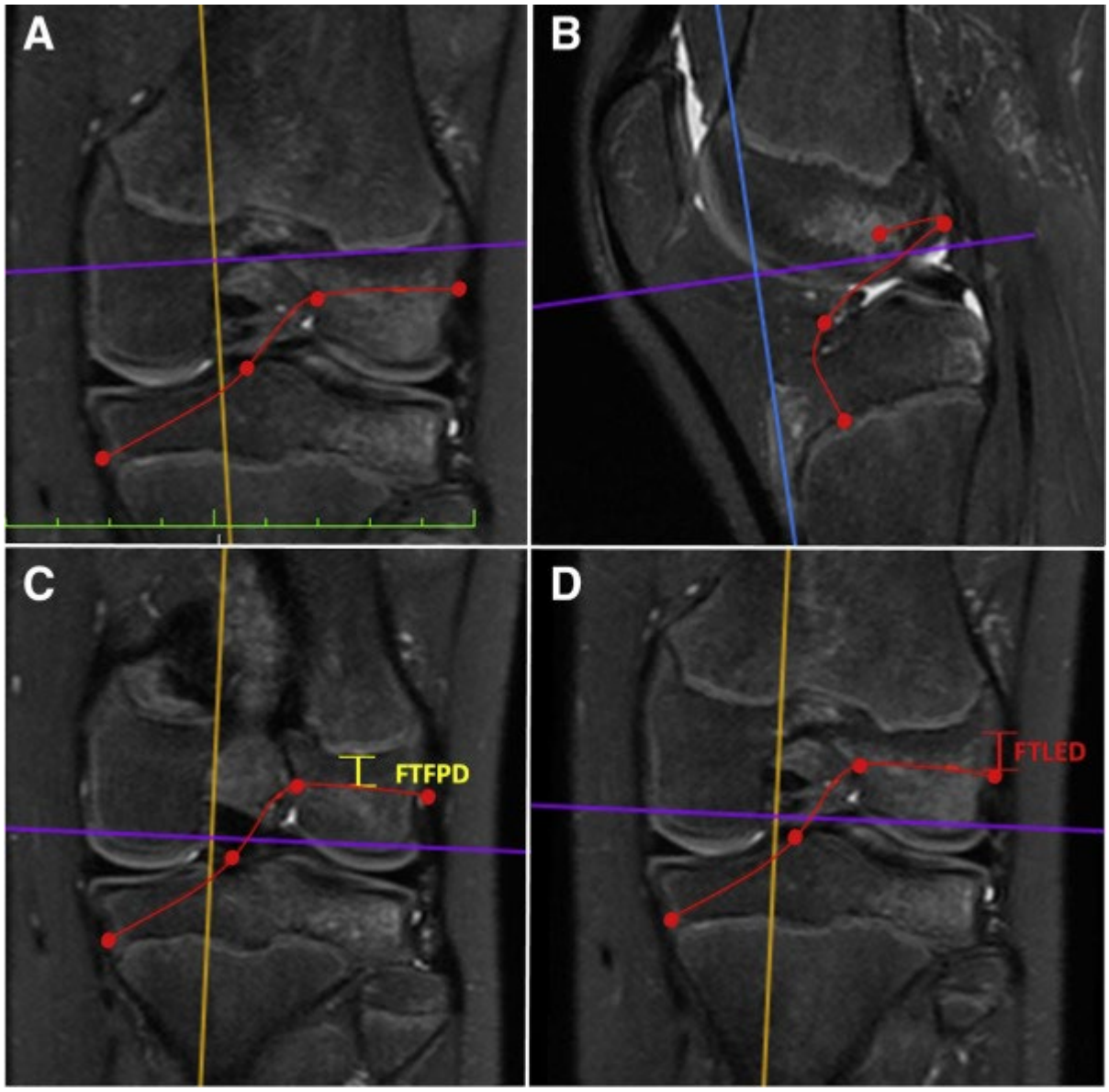

Fig 3. Three-dimensional (3D) measurements performed on the 3D magnetic resonance imaging of a left knee. All-inside all-epiphyseal pediatric anterior cruciate ligament reconstruction on (A) coronal and (B) sagittal cuts. In addition, on the coronal cuts, the (C) femoral tunnel – femoral physis distance (FTFPD, yellow line) and the (D) femoral tunnel – lateral femoral epicondyle distance (FTLED, red line) were measured.

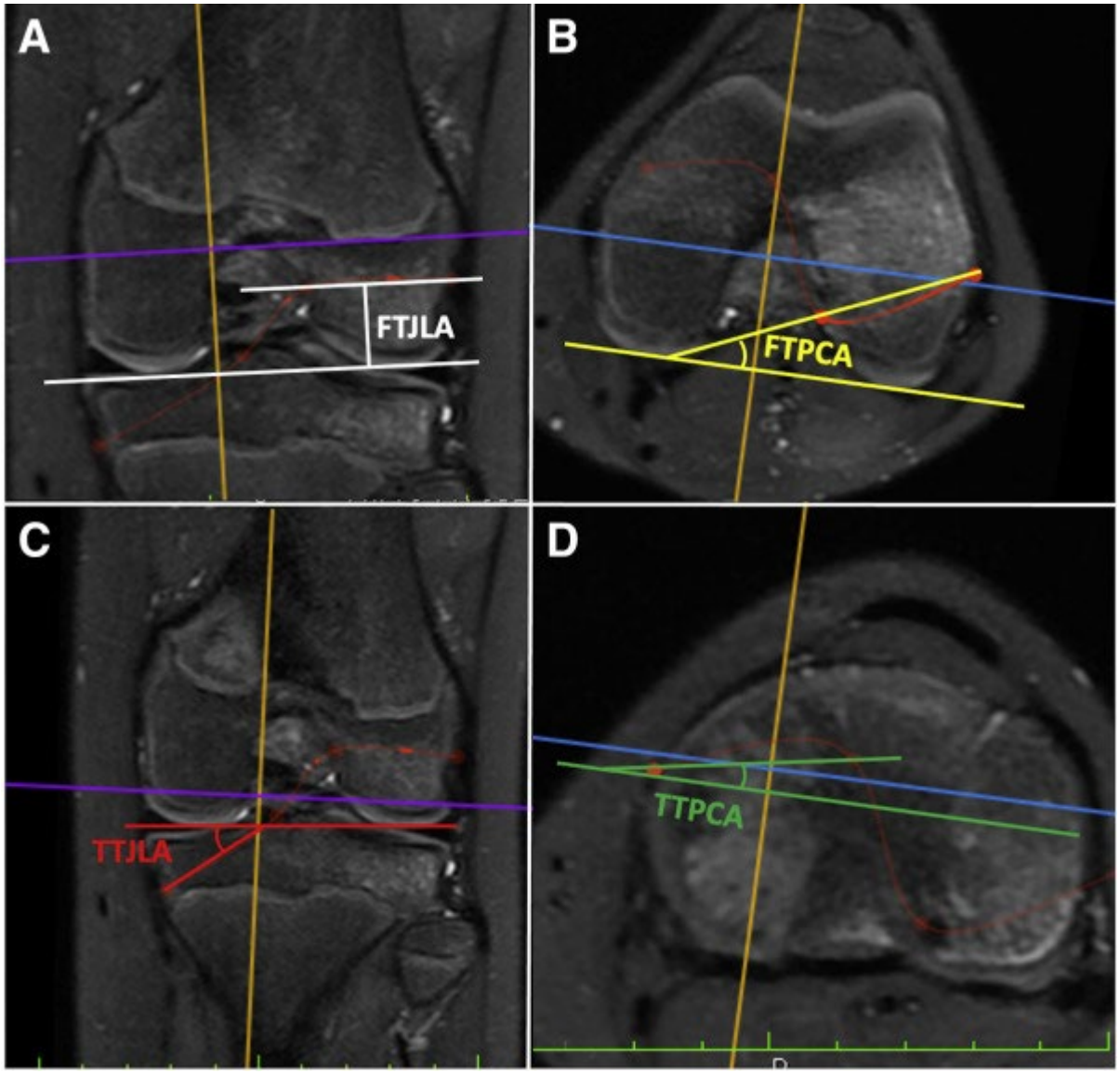


Fig 4. Three-dimensional (3D) measurements performed on the 3D magnetic resonance imaging sequences of a left knee. (A) Femoral tunnel / joint line angle (FTJLA, white line) measured on the coronal plane. Both observers decided that a tunnel parallel to the joint line was the only safe way to place the femoral tunnel. (B) Femoral tunnel / posterior condylar axis angle (FTPCA, yellow line) measured on the axial plane. (C) Tibial tunnel / joint line angle (TTJLA, red line) measured on the coronal plane. (D) Tibial tunnel / posterior condylar axis angle (TTPCA, green line) measured on the axial plane.

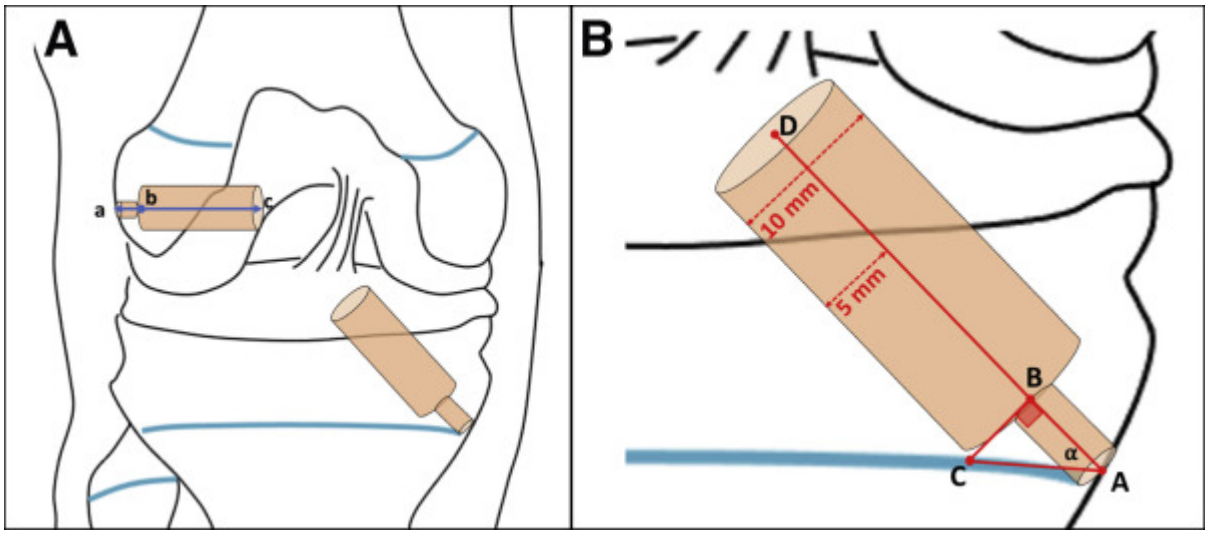


Fig 5. Schematic drawing of the femoral and tibial tunnels measured for the all-inside all-epiphyseal pediatric anterior cruciate liagment reconstruction. (A) The segment ac is the femoral full tunnel, the segment bc is the femoral socket, and the segment ab is the safe zone of lateral femoral cortex for suspensory fixation and was set at 5 mm. (B) The segment AD is the tibial full tunnel, the segment DB is the tibial socket, and the segment AB is the safe zone in order to preserve the proximal tibial physis when retrodrilling a 10-mm tibial socket. The trigonometric formula used to calculate AB was: AB = 5/TAN(α).

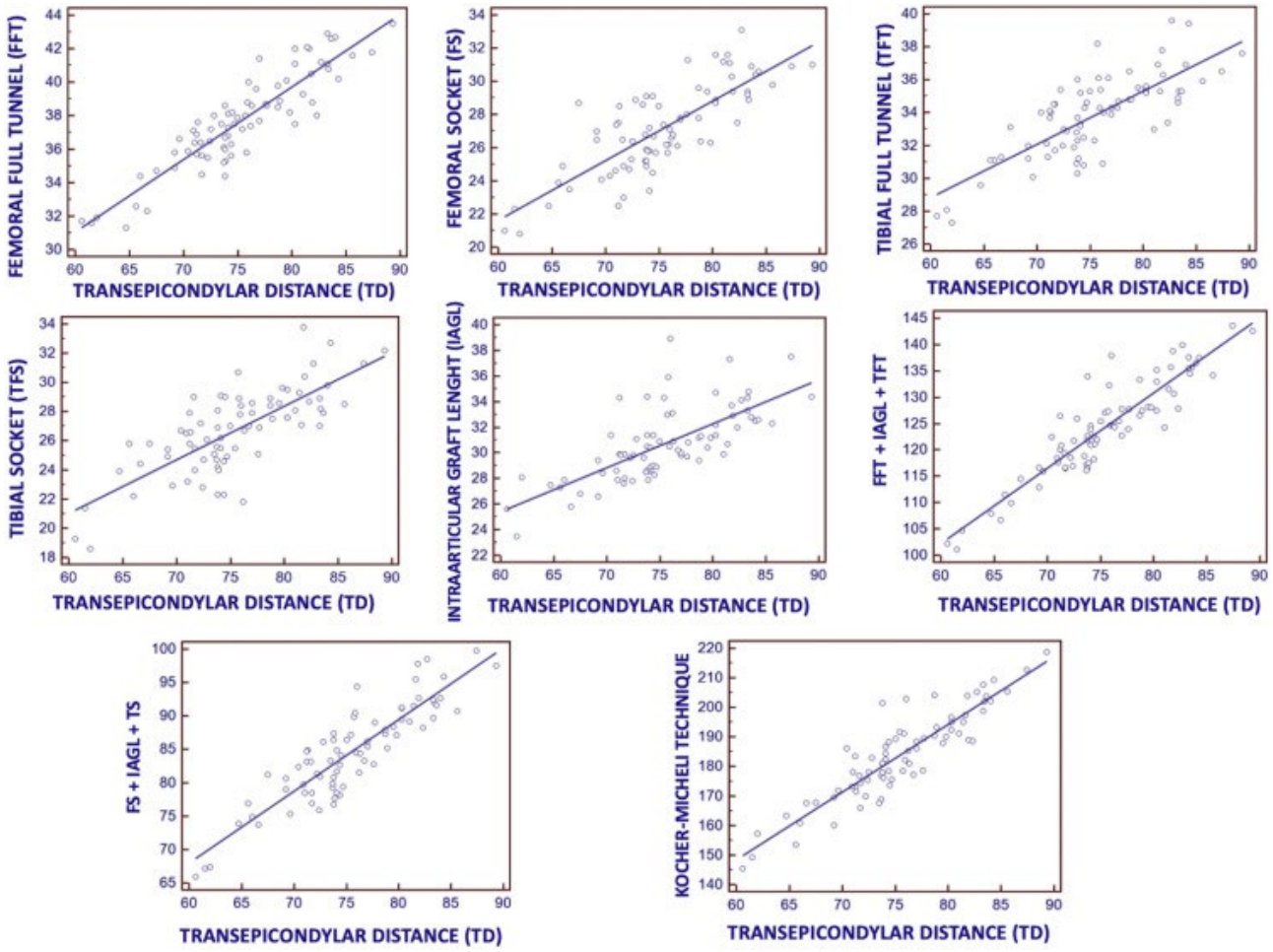

Fig 6. Simple linear regression used to develop mathematical formulas to calculate the 3-dimensional (3D) measurements (Y variable) from the transepicondylar distance (X variable). A linear correlation was found between the transepicondylar distance and all 3D measurements. (FFT, femoral full tunnel; FS, femoral socket; IAGL, intra-articular length of the graft; TD, transepicondylar distance; TFT, tibial full tunnel; TS, tibial socket.)

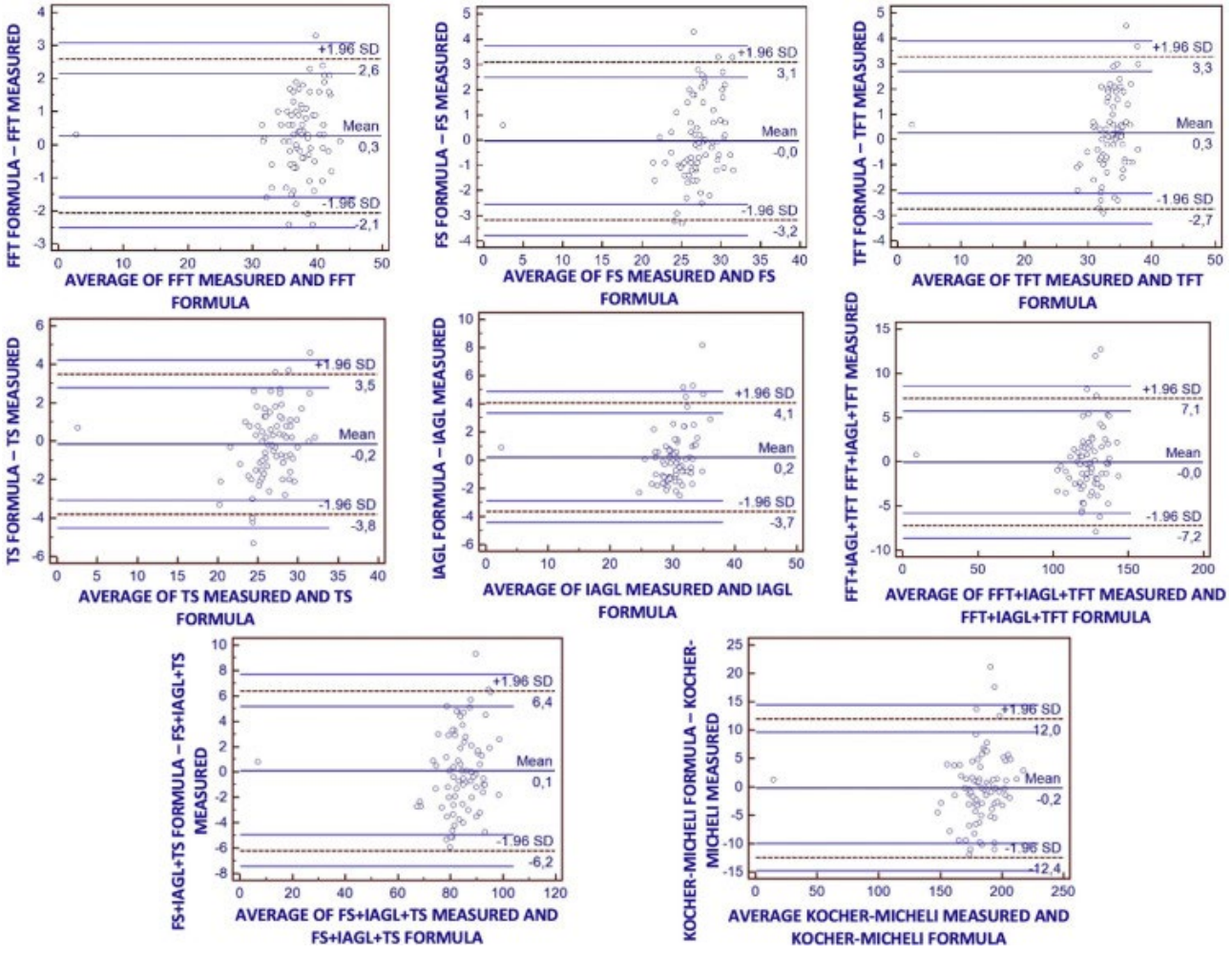


Fig 7. Bland–Altman plots to compare 3-dimensional measurements performed on the magnetic resonance imaging and calculated with the formulas. Abbreviations: (FFT, femoral full tunnel; FS, femoral socket; IAGL, intra-articular length of the graft; TD, transepicondylar distance; TFT, tibial full tunnel; TS, tibial socket.)

**Table 1.** Reference Chart for Surgeons: Length of Tunnels and Grafts for All-Epiphyseal Pediatric ACL Reconstruction and Kocher–Micheli Techniques

| Reference Chart | Length, mm | | | | | | | | |
|---|---|---|---|---|---|---|---|---|---|
| | All-Inside All-Epiphyseal ACL Reconstruction | | | | | | | | Kocher–Micheli |
| Transepicondylar distance (TD) | Intra-articular Length of the Graft (IAGL) | Maximum Length of the Femoral Socket (FS) | Maximum Length of the Tibial Socket (TS) | Maximum Length of FS + IAGL + TS | Maximum Graft Length (FS+IAGL+TS) − 5 mm | Recommended Length of the Femoral Socket (RFS) | Recommended Length of the Tibial Socket (RTS) | Recommended Graft's Length (RFS+IAGL+RTS) − 5 mm | Recommended Length of the Iliotibial Band Graft |
| 60-65 mm | 25 | 21 | 21 | 67 | 62 | 20 | 20 | 60 | 170 |
| 65.1-70 mm | 27 | 23 | 23 | 73 | 68 | 20 | 20 | 62 | 181 |
| 70.1-75 mm | 28 | 25 | 24 | 77 | 72 | 20 | 20 | 63 | 193 |
| 75.1-80 mm | 30 | 27 | 26 | 83 | 78 | 25 | 25 | 75 | 204 |
| 85.1-85 mm | 32 | 28 | 28 | 88 | 83 | 25 | 25 | 77 | 216 |
| 85.1-90 mm | 33 | 30 | 30 | 93 | 88 | 25 | 25 | 78 | 227 |

ACL, anterior cruciate ligament.

**Appendix Table 1.** Summary of Parameters Measured, Intra-Observer and Inter-Observer Reliability

| | Observer 1 | | | | Observer 2 | | | | | | |
|---|---|---|---|---|---|---|---|---|---|---|---|
| | Time 0 | | Time 1 | | Time 0 | | Time 1 | | Observer 1 (T0 + T1) + Observer 2 (T0 +T1) | | |
| Parameter Measured, mm | Mean | SD | Mean | SD | Mean | SD | Mean | SD | Mean | SD | Range |
| 2D measurements | | | | | | | | | | | |
| Transepicondylar distance (TD) | 75.4 | 5.9 | 75.2 | 5.9 | 75.6 | 6.0 | 75.3 | 6.2 | 75.4 | 6.0 | 60.6-89.3 |
| Proximal tibia mediolateral dimension (PTML) | 69.1 | 6.5 | 69.0 | 6.5 | 69.7 | 6.2 | 69.0 | 6.1 | 69.2 | 6.2 | 53.8-81.3 |
| Tibial plateau anteroposterior dimension (TAP) | 41.5 | 4.9 | 41.1 | 5.2 | 41.4 | 4.4 | 42.3 | 4.9 | 41.6 | 4.6 | 31-51.3 |
| Lateral femoral condyle anteroposterior dimension (LFAP) | 55.7 | 6.4 | 55.1 | 7.0 | 55.3 | 7.0 | 55.6 | 6.5 | 55.4 | 6.3 | 40-69.2 |
| Lateral femoral condyle medio-lateral dimension (LFML) | 29.2 | 2.9 | 29.9 | 3.2 | 30.9 | 3.3 | 30.6 | 3.2 | 30.1 | 2.9 | 22.5-35.6 |
| Lateral femoral condyle craniocaudal dimension (LFCD) | 23.0 | 2.8 | 23.0 | 2.9 | 24.7 | 3.2 | 24.8 | 3.3 | 23.9 | 2.9 | 16.2-30.8 |
| Medial femoral condyle cranio-caudal dimension (MFCD) | 29.5 | 3.5 | 29.2 | 5.0 | 30.2 | 3.6 | 30.3 | 3.5 | 29.8 | 3.6 | 20.8-37.3 |
| 3D measurements | | | | | | | | | | | |
| All-inside, all-epiphyseal ACL reconstruction | | | | | | | | | | | |
| Femoral full tunnel (FFT) | 33.0 | 3.0 | 32.5 | 2.9 | 31.6 | 3.2 | 31.4 | 3.2 | 32.1 | 2.7 | 25.8-38.1 |
| Femoral tunnel – lateral epicondyle distance (FTLED) | 10.8 | 1.6 | 11.4 | 1.8 | 10.4 | 1.9 | 10.3 | 1.8 | 10.7 | 1.3 | 8-13.7 |
| Femoral tunnel – femoral physis distance (FTFPD) | 10.2 | 1.6 | 10.8 | 1.7 | 9.6 | 1.9 | 9.3 | 2.0 | 10.0 | 1.4 | 7-12.9 |
| Intra-articular length of the graft (IAGL) | 28.7 | 3.7 | 31.0 | 3.5 | 31.8 | 3.7 | 31.2 | 3.1 | 30.7 | 2.9 | 23.5-38.9 |
| Tibial full tunnel (TFT) | 31.9 | 2.8 | 25.6 | 3.0 | 34.8 | 3.1 | 27.8 | 3.4 | 26.7 | 2.9 | 18.6-33.8 |
| Kocher–Micheli technique | 186.4 | 15.9 | 185.9 | 15.9 | 183.6 | 14.9 | 181.2 | 14.8 | 183.7 | 15.0 | 145.5-218.7 |

| | Pearson Correlation Index | | | | Spearman Rank Correlation Coefficient | | | | Cronbach Alpha | | | |
|---|---|---|---|---|---|---|---|---|---|---|---|---|
| | Observer 1 | | Observer 2 | | Observer 1 | | Observer 2 | | Observer 1 | | Observer 2 | |
| Intraobserver Reliability | *r* coeff | *P* Value | *r* coeff | *P* Value | rho | *P* Value | rho | *P* Value | Alpha | CI 95% | Alpha | CI 95% |
| 2D measurements | | | | | | | | | | | | |
| Transepicondylar distance (TD) | 1.00 | <.0001 | .98 | <.0001 | – | – | – | – | 1.00 | 1.00 | .99 | .98 |
| Proximal tibia mediolateral dimension (PTML) | .98 | <.0001 | .95 | <.0001 | – | – | – | – | .99 | .98 | .98 | .96 |
| Tibial plateau anteroposterior dimension (TAP) | – | – | .88 | <.0001 | .91 | <.0001 | – | – | .93 | .89 | .94 | .91 |
| Lateral femoral condyle anteroposterior dimension (LFAP) | – | – | – | – | .83 | <.0001 | .94 | <.0001 | .91 | .87 | .93 | .91 |
| Lateral femoral condyle mediolateral dimension (LFML) | .82 | <.0001 | .89 | <.0001 | – | – | – | – | .90 | .85 | .94 | .91 |
| Lateral femoral condyle cranio–caudal dimension (LFCD) | .93 | <.0001 | .95 | <.0001 | – | – | – | – | .96 | .94 | .98 | .96 |
| Medial femoral condyle cranio–caudal dimension (MFCD) | – | – | .97 | <.0001 | 0.64 | <.0001 | – | – | 0.78 | 0.68 | .99 | .98 |
| 3D measurements | | | | | | | | | | | | |
| All–inside, all–epiphyseal ACL reconstruction | – | – | – | – | – | – | – | – | – | – | – | – |
| Femoral full tunnel (FFT) | .84 | <.0001 | .64 | <.0001 | – | – | – | – | .92 | .88 | 0.78 | 0.68 |

**Appendix Table 1.** Continued

| | Pearson Correlation Index | | | | Spearman Rank Correlation Coefficient | | | | Cronbach Alpha | | | |
|---|---|---|---|---|---|---|---|---|---|---|---|---|
| | Observer 1 | | Observer 2 | | Observer 1 | | Observer 2 | | Observer 1 | | Observer 2 | |
| Intraobserver Reliability | *r* coeff | *P* Value | *r* coeff | *P* Value | rho | *P* Value | rho | *P* Value | Alpha | CI 95% | Alpha | CI 95% |
| Femoral tunnel – lateral epicondyle distance (FTLED) | 0.47 | <.0001 | .31 | .01 | – | – | – | – | 0.64 | 0.47 | 0.48 | 0.24 |
| Femoral tunnel – femoral physis distance (FTFPD) | 0.57 | <.0001 | .50 | <.0001 | – | – | – | – | 0.73 | 0.60 | 0.67 | 0.51 |
| Intra-articular length of the graft (IAGL) | – | – | – | – | 0.78 | <.0001 | 0.45 | <.0001 | .90 | .86 | 0.62 | 0.44 |
| Tibial full tunnel (TFT) | 0.63 | <.0001 | 0.64 | <.0001 | – | – | – | – | 0.78 | 0.67 | 0.78 | 0.68 |
| Kocher–Micheli technique | .96 | <.0001 | .95 | <.0001 | – | – | – | – | .98 | .97 | .97 | .97 |

| Interobserver Reliability | Intraclass Correlation Coefficient (ICC) | | | | Cronbach Alpha | Cronbach Alpha |
|---|---|---|---|---|---|---|
| | Single Measures | 95% CI | Average Measures | 95% CI | Obs 1 (T1) and Obs 2 (T1) Alpha | 95% CI |
| 2D measurements | | | | | | |
| Transepicondylar distance (TD) | 0.9916 | 0.9869-0.9947 | .9958 | 0.9934-0.9973 | 0.9961 | 0.9942 |
| Proximal tibia medio −lateral dimension (PTML) | 0.9713 | 0.9550-0.9817 | .9854 | 0.9770-0.9908 | 0.9864 | 0.9801 |
| Tibial plateau anteroposterior dimension (TAP) | 0.9295 | 0.8910-0.9547 | 0.9635 | 0.9423-0.9768 | 0.9645 | 0.984 |
| Lateral femoral condyle anteroposterior dimension (LFAP) | 0.9136 | 0.8670-0.9444 | 0.9548 | 0.9288-0.9714 | 0.9549 | 0.9339 |
| Lateral femoral condyle mediolateral dimension (LFML) | 0.7983 | 0.6993-0.8673 | 0.8879 | 0.8230-0.9289 | 0.8901 | 0.839 |
| Lateral femoral condyle craniocaudal dimension (LFCD) | 0.9087 | 0.8596-0.9411 | 0.9522 | 0.9245-0.9697 | 0.9571 | 0.9371 |
| Medial femoral condyle craniocaudal dimension (MFCD) | 0.8538 | 0.7787-0.9048 | 0.9211 | 0.8756-0.9500 | 0.9226 | .8866 |
| 3D measurements | | | | | | |
| All-inside, all-epiphyseal ACL reconstruction | | | | | | |
| Femoral full tunnel (FFT) | 0.7637 | 0.6510-0.8435 | 0.866 | 0.7886-0.9151 | 0.8661 | 0.8037 |
| Femoral tunnel-lateral epicondyle distance (FTLED) | 0.533 | 0.3570-0.6763 | 0.6953 | 0.5193-0.8069 | 0.6957 | 0.5541 |
| Femoral tunnel-femoral physis distance (FTFPD) | 0.6164 | 0.4551-0.7385 | 0.7627 | 0.6255-0.8496 | 0.7691 | 0.6615 |
| Intra-articular length of the graft (IAGL) | 0.6269 | 0.4686-0.7462 | 0.7707 | 0.6381-0.8547 | 0.7784 | 0.6752 |
| Tibial full tunnel (TFT) | 0.7488 | 0.6305-0.8331 | 0.8564 | 0.7733-0.9090 | 0.8573 | 0.7909 |
| Kocher−Micheli technique | 0.9378 | 0.9036-0.9601 | 0.9679 | 0.9494-0.9797 | 0.9688 | 0.9543 |

NOTE. Parameter measured: Summary of the 2D and 3D measurements in mm for the 2 observers at Time 0 and Time 1 (30 days after Time 0). The last column includes the mean and SD obtained from the sum of Observer 1 (Time 0) + Observer 1 (Time 1) + Observer 2 (Time 0) + Observer 2 (Time 1).

Intraobserver reliability: Pearson or Spearman correlation according to the normality of the data distribution and Cronbach alpha for the 2D and 3D measurements.

Interobserver reliability: tested with Intraclass correlation coefficient (ICC) and Cronbach alpha for the 2D and 3D measurements. The second measurement (T1) of each observer was used for every test.

2D, 2-dimensional; 3D, 3-dimensional; ACL, anterior cruciate ligament; CI, confidence interval; coeff, coefficient; Obs, observer; SD, standard deviation.

**Appendix Table 2.** Correlation Between 2D Measurements (Independent Variables) And 3D Measurements (Dependent Variables)

| Correlation Between 2D and 3D Variables | Dependent Variables (3D Measurements) | | | | | | | | | | | |
|---|---|---|---|---|---|---|---|---|---|---|---|---|
| | Femoral Full Tunnel (FFT) | | Femoral Tunnel-Lateral Epicondyle Distance (FTLED) | | Femoral Tunnel-Femoral Physis Distance (FTFPD) | | Intra-Articular Length of the Graft (IAGL) | | Tibial Full Tunnel (TFT) | | Kocher−Micheli Technique | |
| Independent Variables (2D Measurements) | r coeff | *P* Value | r coeff | *P* Value | r coeff | *P* Value | r coeff | *P* Value | r coeff | *P* Value | r coeff | *P* Value |
| Transepicondylar distance (TD) | 0.7983 | <.0001 | 0.7165 | <.0001 | 0.6512 | <.0001 | 0.6808 | <.0001 | 0.7781 | <.0001 | .9073 | <.0001 |
| Proximal tibia mediolateral dimension (PTML) | 0.7432 | <.0001 | 0.6787 | <.0001 | 0.5911 | <.0001 | 0.7311 | <.0001 | 0.7518 | <.0001 | .9012 | <.0001 |
| Tibial plateau anteroposterior dimension (TAP) | 0.6828 | <.0001 | 0.5976 | <.0001 | 0.6038 | <.0001 | 0.7342 | <.0001 | 0.6845 | <.0001 | .9001 | <.0001 |
| Lateral femoral condyle anteroposterior dimension (LFAP) | 0.5669 | <.0001 | 0.5751 | <.0001 | 0.5232 | <.0001 | 0.673 | <.0001 | 0.6357 | <.0001 | .8625 | <.0001 |
| Lateral femoral condyle mediolateral dimension (LFML) | 0.787 | <.0001 | 0.5598 | <.0001 | 0.5108 | <.0001 | 0.5155 | <.0001 | 0.698 | <.0001 | 0.7646 | <.0001 |
| Lateral femoral condyle craniocaudal dimension (LFCD) | 0.5669 | <.0001 | 0.7522 | <.0001 | 0.7392 | <.0001 | 0.7481 | <.0001 | 0.6843 | <.0001 | .8743 | <.0001 |
| Medial femoral condyle craniocaudal dimension (MFCD) | 0.5238 | <.0001 | 0.6262 | <.0001 | 0.5894 | <.0001 | 0.731 | <.0001 | 0.6514 | <.0001 | .8221 | <.0001 |

NOTE. The Pearson test was used (all data normally distributed).

2D, 2-dimensional; 3D, 3-dimensional; ACL, anterior cruciate ligament; coeff, coefficient.